Hermolin, J., Gallant, J., & Fillingame, R. H. (1983) *J. Biol. Chem. 258*, 14550–14555.
Hochman, Y., & Carmeli, C. (1981) *Biochemistry 20*, 6287–6292.
Hundal, T., Norling, B., & Ernster, L. (1983) *FEBS Lett. 162*, 5–10.
Issartel, J.-P., Lunardi, J., & Vignais, P. V. (1986) *J. Biol. Chem. 261*, 895–901.
Jacobs, E. E., Jacobs, M., Sanadi, D. R., & Bradley, L. B. (1956) *J. Biol. Chem. 223*, 147–156.
Khananshvili, D., & Gromet-Elhanan, Z. (1984) *FEBS Lett. 178*, 10–14.
Khananshvili, D., & Gromet-Elhanan, Z. (1985) *Proc. Natl. Acad. Sci. U.S.A. 82*, 1886–1890.
Kironde, F. A., & Cross, R. L. (1987) *J. Biol. Chem. 262*, 3488–3495.
Liang, A. M., & Fisher, R. J. (1983) *J. Biol. Chem. 258*, 4788–4793.
Lowry, O. H., Rosebrough, N. J., Farr, A. L., & Randall, R. J. (1951) *J. Biol. Chem. 193*, 265–275.
Moyle, J., & Mitchell, P. (1975) *FEBS Lett. 56*, 55–61.
Ovchinnikov, Y. A., Modyanov, N. N., Grinkevich, V. A., Belogrudov, G. I., Hundal, T., Norling, B., Sandri, G., Wojtczak, L., & Ernster, L. (1985) in *Achievements and Perspectives of Mitochondrial Research* (Quagliariello, E., et al., Eds.) Vol. 1, pp 223–236, Elsevier, New York.
Pedersen, P. L., & Hullihen, J. (1978) *J. Biol. Chem. 253*, 2176–2183.
Pedersen, P. L., & Hullihen, J. (1979) *Methods Enzymol. 55*, 736–741.
Penin, F., Deleâge, G., Godinot, C., & Gautheron, D. C. (1986) *Biochim. Biophys. Acta 852*, 55–67.
Pullman, M. E., Penefsky, H. S., Datta, A., & Racker, E. (1960) *J. Biol. Chem. 235*, 3322–3329.
Racker, E. (1977) *Annu. Rev. Biochem. 46*, 1006–1013.
Selwyn, M. J. (1967) *Biochem. J. 105*, 279–288.
Senior, A. E. (1973) *Biochim. Biophys. Acta 301*, 249–277.
Senior, A. E. (1979) *J. Biol. Chem. 254*, 11319–11322.
Senior, A. E., & Wise, J. G. (1983) *J. Membr. Biol. 73*, 105–124.
Senior, A. E., Richardson, L. V., Baker, K., & Wise, J. G. (1980) *J. Biol. Chem. 255*, 7211–7217.
Shavit, N., Conrad, Z., & Yoshida, M. (1986) *Fourth European Bioenergetics Conference (Short Reports)*, Vol. 4, p 274, Prague, Czechoslovakia.
Stezowski, J. J., & Hoard, J. L. (1984) *Isr. J. Chem. 24*, 323–334.
Vadineau, A., Berden, J. A., & Slater, E. C. (1976) *Biochim. Biophys. Acta 449*, 468–479.
Wang, J. H. (1983) *Annu. Rev. Biophys. Bioeng. 12*, 21–24.
Weber, K., & Osborn, M. (1969) *J. Biol. Chem. 244*, 4406–4412.
Williams, N., & Coleman, P. S. (1982) *J. Biol. Chem. 257*, 2834–2841.
Williams, N., Hullihen, J., & Pedersen, P. L. (1984) *Biochemistry 23*, 780–785.
Williams, N., Hullihen, J., & Pedersen, P. L. (1987) *Biochemistry 26*, 162–169.
Wise, J. G., Duncan, T. M., Latchney, L. R., Cox, D. N., & Senior, A. E. (1983) *Biochem. J. 215*, 343–350.

Probing of Sulfhydryl Groups in the Adenosine 5′-Diphosphate/Adenosine 5′-Triphosphate Carrier by Maleimide Spin-Labels†

Anton Munding, Michael Drees, Klaus Beyer,* and Martin Klingenberg
Institut für Physikalische Biochemie, Universität München, Goethestrasse 33, 8000 München 2, FRG
Received March 11, 1987; Revised Manuscript Received September 1, 1987

ABSTRACT: Binding of spin-labeled maleimides to the mitochondrial ADP/ATP carrier was investigated both in mitochondria and in the detergent-solubilized carrier protein. In mitochondria, spin-label binding to the carrier was evaluated by preincubation with the inhibitor carboxyatractyloside. The membrane sidedness of SH groups in the carrier molecule was determined by chemical reduction of nitroxides on the cytosolic membrane surface by Fe^{2+} or by pretreatment of the mitochondria with impermeant SH reagents. These experiments suggest that each subunit of the dimeric carrier incorporates one spin-labeled maleimide. Roughly half of the carrier-bound spin-labels were found on either side of the mitochondrial membrane. The detergent-solubilized carrier protein was labeled with a series of maleimide derivatives containing a spacer of increasing length between the maleimide and nitroxide moieties. A total spin-label binding of 2–3 mol/mol of protein dimer, depending on the spin-label length, was found. The electron spin resonance spectra of the spin-labeled protein invariably showed strongly and weakly immobilized components. Increasing the distance of the nitroxide from the maleimide ring resulted in a strong increase of the contribution of the weakly immobilized component. These observations led to the conclusions that the geometrical constraint of spin-label mobility changes at a distance of about 10 Å from the maleimide binding site.

Two conformational states linked to the orientation of the binding center of the mitochondrial ADP/ATP carrier (AAC)[1]—specified as the c and m state, respectively—have been defined by the transport inhibitors atractylate and bongkrekate (Weidemann et al., 1969; Erdelt et al., 1972). Under specific conditions, the ADP/ATP exchange can be

† The ESR instrument was purchased with a grant from the Deutsche Forschungsgemeinschaft (Be 828/2). Also, the work was supported by the Deutsche Forschungsgemeinschaft.
* Address correspondence to this author.

[1] Abbreviations: AAC, ADP/ATP carrier; ATR, atractylate; CAT, carboxyatractyloside; BKA, bongkrekic acid; NEM, *N*-ethylmaleimide; MOPS, 4-morpholinepropanesulfonic acid; EDTA, ethylenediaminetetraacetic acid; MSL, maleimide spin-label; DTNB, 5,5′-dithiobis(2-nitrobenzoic acid); PCMB, *p*-(chloromercuri)benzoate; ESR, electron spin resonance.

0006-2960/87/0426-8637$01.50/0

Chart I

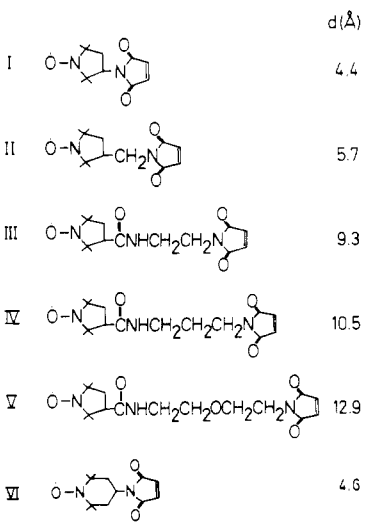

inhibited by sulfhydryl reagents (Leblanc & Clauser, 1972; Vignais & Vignais, 1972; Aquila et al., 1982a). This inhibition by *N*-ethylmaleimide (NEM) was found to depend on the presence of ADP or ATP, which indicated that the SH group was reactive only in the m state (Klingenberg, 1976). In accordance, the binding of NEM to the AAC was shown to be suppressed by atractylate (ATR) or carboxyatractylate (CAT), whereas in the presence of bongkrekate (BKA) two SH groups in the dimeric protein can react with NEM (Aquila & Klingenberg, 1982). Also, ADP stimulated the incorporation of the SH reagents into the carrier molecule.

Although the total maleimide binding to the AAC and the relationship between protein rearrangement and SH unmasking have been successfully studied by radioactive NEM, the sidedness of the reactive SH groups and the polarity of their environment have remained in debate (Müller et al., 1984; Houstek & Pedersen, 1985). Spin-label derivatives of the maleimides are suitable for solving these problems. A completely analogous binding behavior to that described earlier for NEM was observed in the present study with spin-labeled maleimides. Thus, it seemed justified to probe the location of sulfhydryl groups by virtue of the sensitivity of the spin-labels to membrane-impermeable reducing agents.

The ESR spectra of spin-labels are very sensitive to motions in the range of 10^{-7}–10^{-9} s. The polarity of the environment of the nitroxyl moiety also influences the spectral shape. Unfortunately, after spin-labeling to mitochondria, ESR spectra are often complex, corresponding in the variety of SH groups in the mitochondrial membrane. In order to make full use of the spin-label method, experiments with the purified protein were performed.

Materials and Methods

Chemicals. The inhibitor CAT was obtained from Sigma and Boehringer, Mannheim. ATR was a gift of Prof. Piozzi (Palermo) and BKA a gift from Prof. W. Berends (Delft). Spin-labeled maleimide derivatives (MSL I–MSL V; cf. Chart I) were purchased from Syva. MSL VI was prepared as described by Rozantsev (1970).

Spin-Labeling of Mitochondria. Beef heart mitochondria were isolated essentially as described by Blair (1967). Spin-labeling was performed by incubation of the freshly prepared mitochondria (5 or 10 mg of mitochondrial protein/mL) in 250 mM sucrose, 10 mM MOPS, 8 mM $MgCl_2$, and 0.5 mM EDTA, pH 7.2 (buffer M), with MSL VI (cf. Chart I) for 5 min at 0 °C. ADP (0.2 mM) was added before MSL incubation in order to facilitate rearrangement of the carrier protein (Aquila & Klingenberg, 1979). If desired, the mitochondria were preincubated with 0.2 mM CAT for 5 min at 0 °C prior to MSL addition. Blocking of sulfhydryl groups on one side of the mitochondrial membrane was achieved by addition of 0.2 mM impermeable sulfhydryl reagents to the mitochondria, followed by the same spin-labeling procedure as described above. Bound MSL was chemically reduced by adding 16 mM $(NH_4)_2Fe(SO_4)_2 \cdot 6H_2O$ and 1.6 mM glutathione to the spin-labeled mitochondria. Thirty seconds after addition of the reductant, the samples were spun down at 12000*g*. After being washed twice with buffer M, the pellets were transferred into 50-μL capillaries. The capillaries were centrifuged for 1 min at 12000*g* in order to enhance the spin density and to obtain equal mitochondrial concentrations.

ESR measurements were completed within 5 min after preincubation with MSL at 0 °C. Spin reduction by the mitochondrial redox system proved to be less than 4% during this time interval.

MSL Binding to the Solubilized Carrier Protein. The ADP/ATP carrier, loaded with [^{3}H]ATR, was isolated in a Triton X-100 containing buffer (100 mM Na_2SO_4, 10 mM MOPS, 0.05 mM EDTA, and 0.05 mM NaN_3, pH 7.2) as described by Aquila and Klingenberg (1982). The protein concentration was adjusted to about 5 mg/mL by pressure dialysis. [^{3}H]ATR was replaced in the presence of 0.4 mM ADP by adding a 10-fold or 20-fold molar excess of CAT or BKA, respectively. The spin-labeled maleimides (MSL I–V, cf. Chart I) were added at a ratio of 0.3 μmol of MSL/mg of protein. Excess MSL was removed by chromatography on a Sephadex G75 column (0.7 × 15 cm). The protein-containing fractions were pressure dialyzed to a final concentration of 3–5 mg protein/mL prior to the ESR measurements.

ESR Measurements. ESR spectra were recorded on a Bruker ER 200 D-A spectrometer equipped with a variable-temperature accessory. Samples were measured in 50-μL glass capillaries with an internal diameter of 0.9 mm. All spectra were obtained with a modulation frequency of 100 KHz, a modulation amplitude of 2.5 G, a sweep width of 100 G, and a microwave power of 5 mW in a TM 110 cavity. The sweep width was calibrated by using the signal of residual Mn^{2+} in SrO (Bolton et al., 1972). Double integration and spectral subtractions were performed with a MINC PDP-11/23 minicomputer.

Results

MSL Labeling of Mitochondria. In a series of exploratory experiments, freshly prepared beef heart mitochondria were spin-labeled with the maleimide derivative of 2,2,6,6-tetramethylpiperidinyl-*N*-oxy, denoted by MSL VI in Chart I. The mitochondria were incubated in the presence of 80 μmol of MSL VI/g of mitochondrial protein, as described in Figure 1. This MSL concentration approximately corresponds to a 4-fold excess over the SH groups in mitochondria as detected by NEM alkylation (Aquila et al., 1982a; Vignais & Vignais, 1972). The ESR spectrum exhibits two components denoted by s and w (Figure 1A). The broad outer signals separated by about 65 G indicate that most of the remaining MSL is immobilized. The small spectral component exhibiting narrower line width and hyperfine splitting could not be reduced further by washing. This signal component, which contributes about 10% to the total spin intensity, may be due to a minor MSL portion bound to soluble proteins in the matrix space. Also, unbound MSL which is trapped in the mitochondrial matrix may contribute to this signal. Moreover, a small narrow signal has also been observed in the detergent-solu-

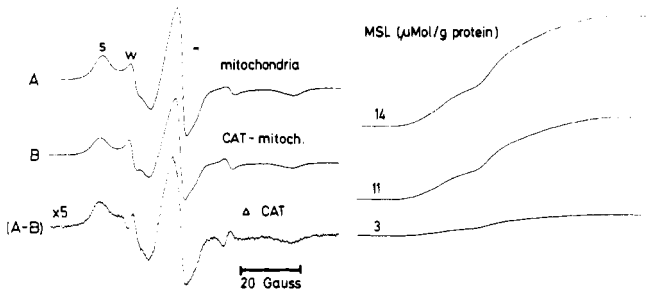

FIGURE 1: ESR spectra of mitochondria after labeling with MSL VI (cf. Chart I). Freshly prepared mitochondria (A) or mitochondria after preincubation with 0.1 mM CAT (B) were incubated with 0.2 mM ADP and 0.8 mM MSL VI at 0 °C for 5 min and washed twice to remove excess spin-label. Concentration of mitochondria, 10 mg of protein/mL. The bottom spectrum (A − B) was obtained by computer subtraction. The two spectral components indicating strong and weak spin-label immobilization are denoted by s and w, respectively. The distorted shape of the residual w component in the difference spectrum probably arises from a slightly larger concentration of MSL bound or trapped in the mitochondrial matrix space in sample B.

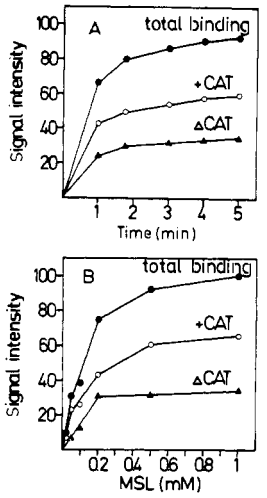

FIGURE 2: (A) Time course of MSL binding to mitochondria without and with CAT preincubation. Mitochondria (10 mg of protein/mL) were spin-labeled with MSL VI (0.8 mM) at 0 °C (see text). The low-field part of the ESR spectra was recorded at different times after spin-label addition, and the line height of the s component was evaluated. (B) Concentration dependence of MSL binding. Mitochondria (10 mg/mL) were spin-labeled with different concentrations of MSL VI. ESR spectra were recorded exactly 5 min after MSL addition and evaluated as in (A). A signal intensity of 100% corresponds to MSL binding obtained 5 min after addition of 1 mM MSL VI to mitochondria.

bilized protein (see below). These potential signal components cannot be distinguished at present.

Preloading of mitochondria at the same protein concentration with CAT resulted in an appreciable reduction of spin-label incorporation. This can be seen more clearly by inspection of the corresponding double integrals in Figure 1. Absolute spin concentrations were determined by comparison with a standard solution of spin-label in aqueous buffer. The total MSL VI binding of about 14 μmol of MSL/g of protein and the reduction of MSL binding by about 29% after addition of CAT to 11 μmol/g of protein compare well with the previously observed CAT-sensitive portion of NEM binding (H. Aquila, private communication).

The rate of MSL incorporation into mitochondria was evaluated at 0 °C with and without CAT (Figure 2A). After incubation of the mitochondrial suspension (10 mg of protein/mL) with MSL VI, the reaction was stopped by rapid centrifugation followed by one washing step. The extent of

Table I: Blocking of Sulfhydryl Groups by Membrane-Impermeable Reagents

preincubation[a]	% of MSL VI binding to mito	% of MSL VI binding to CAT−mito	ΔCAT
	100	71.1	28.9
DTNB	57.3	39.7	17.6
PCMB	57.7	36.5	21.2
mersalyl	78.9	63.2	15.7
NEM	20.4	13.2	7.2

[a] Mitochondria (mito) (5 mg of protein/mL) were incubated with a 0.2 mM aliquot of the SH reagents for 2 min at 0 °C. For further details, see Materials and Methods.

MSL binding was obtained from the amplitude of the broadened low-field signal. These signal amplitudes were related to the corresponding line height at a MSL concentration of 1 mM after 5 min of incubation (cf. Figure 2B). Under the conditions given in Figure 2A, about 90% of the reaction proceeds within 2 min after addition of MSL VI. It seems that in the absence of CAT the carrier-specific SH groups are alkylated by MSL VI at a similar rate as the majority of the SH groups in the mitochondrial membrane. In another experiment, mitochondria at the same concentration as in Figure 1A were incubated with increasing MSL concentrations for 5 min (Figure 2B). The difference between binding with and without CAT pretreatment shows that the carrier sites are saturated at about 0.2 mM MSL VI, corresponding to a binding of 20 μmol of MSL VI/g of protein.

In summary, these experiments show that the reaction of spin-labeled maleimides with mitochondrial SH groups quantitatively resembles the behavior of NEM as detailed in the earlier studies (Aquila et al., 1982a; Vignais et al., 1975). The level of incorporation indicates that the spin-label traverses the mitochondrial membrane as easily as NEM. The decrease by 30% in the presence of CAT is in line with the previously reported mutual exclusion of CAT and NEM binding to the AAC.

Sidedness of MSL Incorporation. On this basis, it was attempted to utilize MSL incorporation to determine the membrane sidedness of the carrier-bound SH groups. In one approach, the "cytosolic" SH groups of mitochondria were blocked by membrane-impermeable SH reagents prior to addition of MSL VI. All incubations were performed under identical conditions (20 μmol of MSL-VI/g of protein; cf. Table I). Again, the residual MSL binding was deduced by double integration of the spectra. Binding to untreated mitochondria was taken as 100%. It can be expected that after pretreatment by impermeable reagents the membrane-permeable spin-label binds only to SH groups facing the matrix space.

From the first two columns in Table I, it follows that DTNB and PCMB prevent about 40% of the spin-label binding in mitochondria, whereas mersalyl seems to be less effective. In contrast, NEM is able to block about 80% of the MSL VI binding sites, in agreement with its known membrane permeability.

The last column in Table I shows the difference in MSL binding between CAT-loaded and unloaded mitochondria. A variable portion of the CAT-sensitive binding—depending on the various SH reagents—is insensitive to the pretreatment with DTNB, PCMB, or mersalyl. With NEM, the CAT difference is reduced, obviously due to penetration of this compound into the membrane and matrix space.

Considerable efforts were invested in an alternative procedure whereby spin-labeled mitochondria were reduced with

Table II: Discrimination between Inside and Outside SH Groups

expt	preincubation[a] with	relative spin intensity[b] no treatment	after Fe^{2+} treatment	difference
1		100	36.1	63.9
	CAT	70.9	21.2	49.7
		difference 29.1	14.9	14.2
2	DTNB	57.3	35.9	21.4
	CAT + DTNB	39.7	25.0	14.7
		difference 17.6	10.9	6.7
3	NEM	20.4	5.7	14.7
	CAT + NEM	13.2	1.5	11.7
		difference 7.2	4.2	3.0

[a] Preincubation time 5 min at 0 °C followed immediately by spin-labeling as described under Materials and Methods. [b] Total double integrals of the spectra are related to the corresponding integral of spin-labeled mitochondria without prelabeling (100%).

membrane-impermeable Fe^{2+} and glutathione, thereby removing the ESR signal of spin-label accessible to the metal ion by rapid chemical reduction. Ruthenium red was added before Fe^{2+} in order to inhibit the possible uptake of the Fe^{2+} ions by the calcium carrier (Reed & Bygrave, 1974). The results of this approach are shown in Table II. CAT was used to differentiate spin-label binding to the AAC against the background as described above. Again, about 30% of the total MSL binding can be assigned to the AAC. The spin-label reduction by Fe^{2+} amounts to 64% in the total and to 50% in the CAT-insensitive MSL VI incorporation. As a result, the double difference gives 14% of MSL VI label directed to the matrix side. This amounts to half of the carrier-bound MSL VI being inaccessible to Fe^{2+} and presumably directed to the matrix side.

In two additional experiments, mitochondria were preincubated with DTNB or NEM before spin reduction. Again, the CAT difference furnished the carrier-specific spin-label binding. Because of the poor penetration of DTNB (see Table I), one could expect that spin-labeling of DTNB-pretreated mitochondria would yield a bound spin intensity identical with that obtained after reduction. However, the ESR signal after DTNB pretreatment was significantly larger than the signal obtained after spin reduction by Fe^{2+} in the first experiment (57.3% vs 36.1%; see Table II, fourth column in experiment 1 and third column in experiment 2).

In DTNB-pretreated mitochondria, Fe^{2+} reduced the spin intensity further, the final value (35.9%) being close to the signal intensity after Fe^{2+} reduction in the absence of DTNB. The difference obtained after DTNB prelabeling and after reduction by Fe^{2+} could be due to incomplete blocking of the SH groups on the cytosolic site of the mitochondrial membrane by DTNB. The concentration of DTNB, PCMB, or mersalyl in these experiments cannot be increased beyond a 2–3-fold excess over the total concentration of SH groups, since membrane damage has been observed at higher ratios. Alternatively, penetration of some Fe^{2+} ions during the incubation and centrifugation intervals cannot be excluded. Indeed, Fe^{2+} uptake was observed with a half-time of about 10 min at 40 mg of protein/mL and 20 mM Fe^{2+} (experiments not shown). It was not possible to follow the kinetics of Fe^{2+} uptake under the incubation conditions of the spin reduction experiments due to the low spin concentration. Therefore, the residual spin intensities corresponding to about 57% (+DTNB) and 36% (+Fe^{2+}) of the total spin-label binding most probably represent upper and lower limits for the MSL portion which is bound to the matrix side of the mitochondrial membrane.

Spin-label reduction upon Fe^{2+} additions is also observed in NEM-pretreated mitochondria. It must be noted that the reaction with NEM proceeds further when mitochondria are preincubated more than 5 min, ultimately leading to total suppression of MSL binding (not shown). In this case, the extensive spin reduction of MSL by Fe^{2+} seems to be due to seepage of the metal ion into the matrix space.

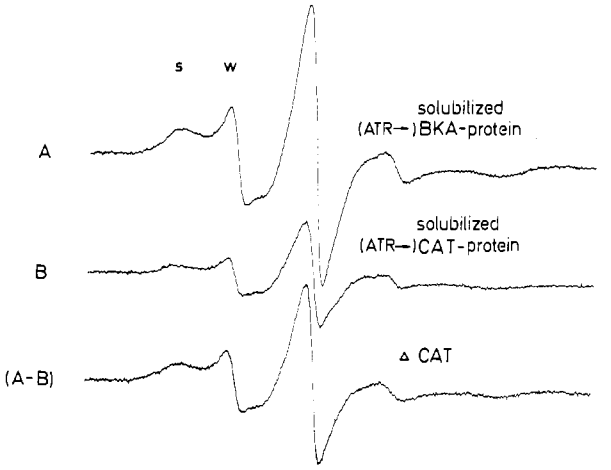

FIGURE 3: ESR spectra of the solubilized carrier protein spin-labeled with MSL III. The ATR–carrier complex (about 5 mg of protein/mL) was incubated at 4 °C for 10 min with 160 μmol of MSL III/g of protein in the presence of ADP (0.4 mM) and BKA (1.6 mM) (spectrum A) or ADP (0.4 mM) and CAT (0.8 mM) (spectrum B). Excess spin-label was removed as described under Materials and Methods. The final protein concentration after pressure dialysis was 4.8 mg of protein/mL. Spectra were recorded at 0 °C. The lower spectrum was obtained by subtracting spectrum B from spectrum A.

Spin-Label Binding to the Isolated AAC. For incorporation of maleimide spin-labels into the solubilized carrier, the isolated ATR–protein complex was used. Although the ATR complex is in the c state (Klingenberg, 1975), it can be rearranged into the m conformation in the presence of ADP and BKA. The protein rearrangement causes release of ATR and, at the same time, binding of BKA (Aquila & Klingenberg, 1979). This is an advantageous method for producing the BKA–carrier complex, since the BKA complex is unstable during the purification steps. For comparison, MSL III (see Chart I) was reacted with both the BKA– and CAT–protein complexes. The spin-label reacts with both inhibitor–protein complexes, however, to a different extent, as shown in Figure 3. Again, two spectral components, denoted by s and w (cf. Figure 1), are observed. However, as mentioned above, in mitochondria, the w component may partially arise from binding to matrix proteins, which are essentially absent in the purified carrier preparation.

In the CAT protein, the carrier-specific SH group as defined in mitochondria should be masked. The "background" binding of MSL III to the CAT protein (cf. spectrum B in Figure 3) was found to be variable among different preparations (not shown). However, the difference between binding to the BKA– and CAT–protein complexes yielded always about 27–31 μmol of MSL/g of protein, as determined by double integration of the difference spectra (bottom spectrum in Figure 3). This corresponds to about two binding sites per protein dimer. This result agrees with the earlier implication that BKA does not block these SH groups (Aquila & Klingenberg, 1979).

The complex binding of MSL to the solubilized carrier protein in its two conformational states can be more clearly visualized by MSL titration as shown in Figure 4. As in the experiment presented in Figure 3, the protein was locked by CAT and BKA in the c or in the m state, respectively. Unlike in Figure 3, excess spin-label was not removed during the

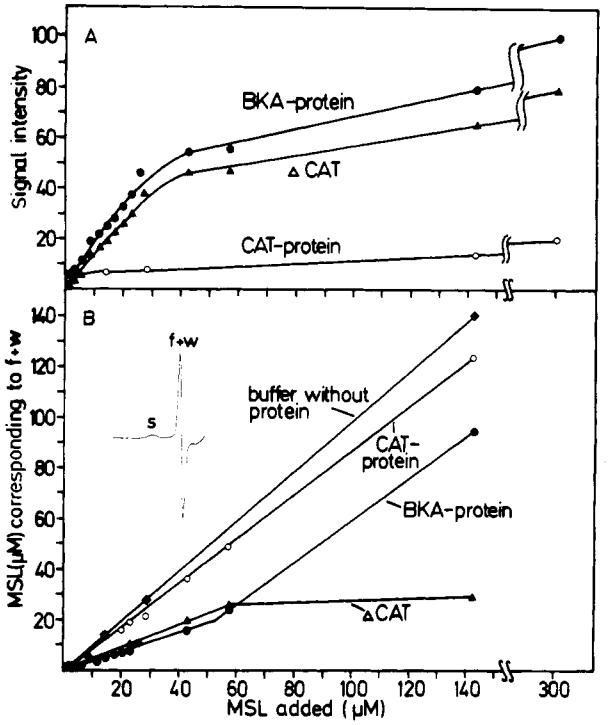

FIGURE 4: Titration of ATR–carrier protein with MSL I. In this experiment, excess MSL was not removed by Sephadex chromatography. The ATR–protein was preincubated with ADP and CAT or BKA as indicated (see Materials and Methods). ESR spectra were recorded 30 min after addition of MSL I at 0 °C. Relative signal amplitudes of the low-field s component (A) and of the low-field f + w component (B) are plotted against total MSL concentration. The difference in signal amplitude between the CAT state and the BKA state is denoted by ΔCAT.

titration. Thus, a narrow three-line ESR spectrum reflecting unbound label is superimposed on the broad signals from the bound MSL portion (see insert in Figure 4B). In Figure 4A, the signal height of the broad low-field spectral component, denoted by s in Figure 3 and in the insert of Figure 4B, is plotted against the total MSL concentration. In the BKA–protein complex, a break appears in the titration curve at about 40 μM added MSL. When CAT protein is titrated analogously, a much smaller increase in the s signal intensity is observed. Moreover, the signal increase appears to be linear in this case.

The distinction between MSL binding to the protein in the CAT and in the BKA states become even more significant (Figure 4B) when the height of the narrow low-field line is evaluated, which represents mainly excess unbound label. It must be noted that this signal masks the narrow line denoted by w in Figure 3. Hence, this signal component is denoted by f + w (cf. insert in Figure 4B). The concentrations given in the ordinate of Figure 4B were calculated by comparing the f + w line heights with standard spectra derived from aqueous solutions of water-soluble spin-labels of known concentration. The corresponding curve obtained with MSL I in buffer without protein is included in Figure 4B. Again, the titration curve in the BKA complex is biphasic, whereas the signal intensity increases linearly in the presence of CAT protein. The slightly reduced slope of the titration curve in the presence of CAT protein as compared to the curve obtained with protein-free buffer may be due to nonspecific MSL binding. Above 60 μM added MSL, the difference between the BKA and CAT curves (ΔCAT) assumes a constant value. Allowing for protein concentration and for the molecular weight of the protein dimer of 67 000 (Aquila et al., 1982b), this value corresponds to about 2 mol of MSL/mol of protein.

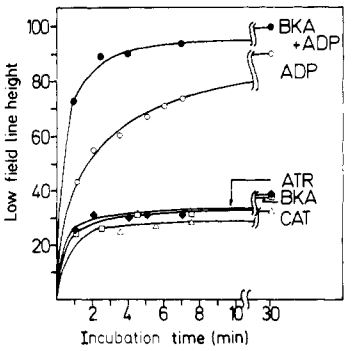

FIGURE 5: Time courses of MSL binding to the solubilized carrier protein in the presence of different ligands. 60 μmol of MSL I/g of protein was added to the ATR–carrier complex (♦) or to the carrier protein after preincubation of the ATR complex for 5 min with 0.8 mM CAT (△), 1.6 mM BKA (□), 0.4 mM ADP (○), or 1.6 mM BKA and 0.4 mM ADP (●). Relative MSL binding, as obtained from the amplitude of the s component (cf. insert in Figure 4B), was arbitrarily set at 100 in the sample containing BKA and ADP after 30 min. All incubations and ESR measurements were performed at 0 °C.

The effect of ADP on the unmasking of sulfhydryl groups is demonstrated in Figure 5. The time course of the c → m interconversion can be conveniently followed by evaluating the peak height of the immobilized spectral component s (cf. Figure 3). The spin-label MSL I was added either directly to the ATR protein or after incubation of the ATR–protein with CAT, BKA, or BKA and ADP as indicated in Figure 5. An increase in spin-label binding was only observed in the presence of ADP. Addition of BKA obviously accelerates the transition of the carrier into the m state. This result clearly corroborates the earlier findings, that the AAC is conformationally fixed in the absence of adenine nucleotides (Klingenberg et al., 1976).

In order to probe the environment of the MSL binding site, we applied maleimide derivatives with spacers between the maleimide and the nitroxide moieties (labels I–V in Chart I). In more favorable cases, this approach allows one to conclude from the change in nitroxide hyperfine splitting with increasing spin-label length that the binding site is embedded in a cleft of certain depth (Hsia & Piette, 1969; Hull et al., 1975; Zeidan et al., 1985). The chain lengths given in Table I and in Figures 6 and 7 refer to the spacer length excluding the nitroxide ring as defined by Hull et al. (1975). After removal of excess spin-label as described above, all spectra exhibited two components (s and w, Figure 6). The total MSL binding in the BKA- and CAT–carrier complexes was evaluated by protein determination and double integration of the whole composite spectra. When CAT is bound to the carrier protein, spin-label binding is low (0.3–0.4 mol/mol of protein), whereas the BKA–protein complex binds 2–3 mol of MSL.

The most obvious feature of the spectra in Figure 6 is the changing ratio of the s and w components with increasing spin-label length. Several experiments were performed in order to influence the s/w signal ratio. Interruption of MSL binding after short incubations revealed no difference in the buildup rate of s and w. Also, the rate of spin reduction by ascorbate was nearly identical for the two components (experiments not shown). A contribution to the w component by MSL trapped in Triton micelles could be excluded. Triton removal or Triton addition to the spin-labeled protein complex had no significant influence on the s/w ratio.

Unfortunately, it was impossible to evaluate the s/w ratios by double integration in terms of spin density ratios since the components were intermingled even at 0 °C. Attempts to separate the two individual components by subtraction of

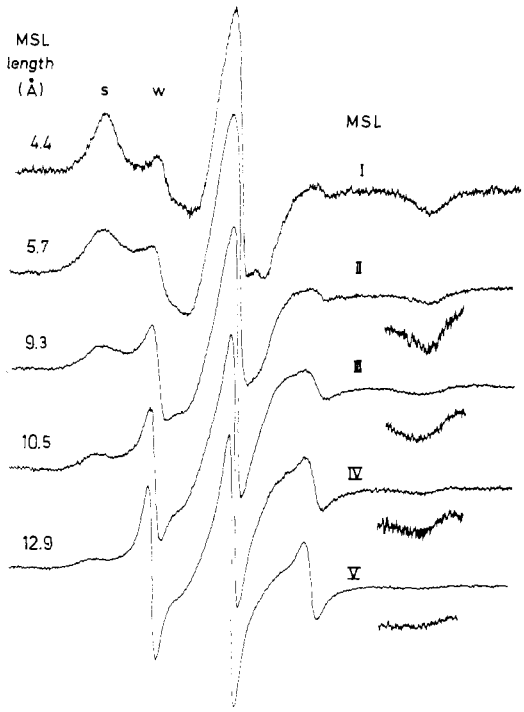

FIGURE 6: ESR spectra of maleimide spin-labels of different length, bound to solubilized carrier protein. ATR protein (3–5 mg of protein/mL) was converted into the m state and spin-labeled with MSL I–V as described under Materials and Methods. Unbound spin-label was removed by Sephadex chromatography. ESR spectra were recorded at 10 °C.

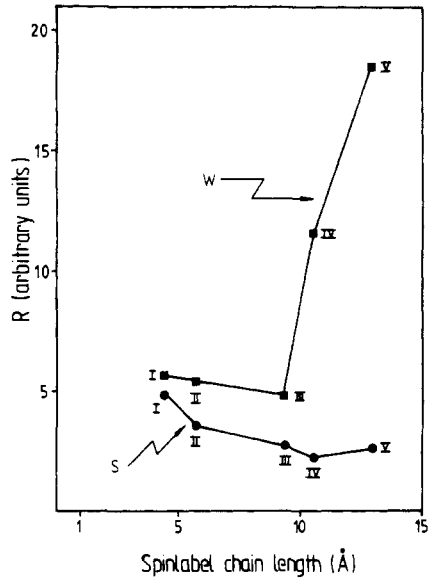

FIGURE 7: Change in the s and w components with MSL chain length as determined by the ratio (R) of the s peak amplitude to the total ESR integral (s) or of the w peak amplitude to the total integral (w).

appropriate spectra of spin-labels in glycerol/water mixtures were not successful as none of these components seemed to fit the spectrum of an isotropically tumbling nitroxide. Also, intersubtractions of different spectra in Figure 6 did not lead to purely isolated s or w components presumably due to very slight differences in the line shapes of s and w among the series of MSL spectra of Figure 6. For the same reason, it is probably difficult to obtain reliable hyperfine splitting values of the spectral components.

Thus, the spectral changes in Figure 6 were analyzed in a more intuitive way by relating the line heights of s and w to the total double integral of the spectra (Figure 7). This procedure provides an approximate measure of the change in the spin density ratio since the change in the line width of s and w on going from the shortest to the longest maleimide spin-label is rather small. Considering the w component, Figure 7 suggests that the environment of the nitroxide changes abruptly at a spacer length of about 9–10 Å. The lack of a corresponding break in the curve from the s component may be due to the overlapping downfield wing of the w signal, which contributes to the s line height.

DISCUSSION

Maleimide Spin-Label Binding to the Carrier Protein in Mitochondria. The present study shows that the inhibitor difference method allows one to study the specific binding of spin-labeled maleimides to the ADP/ATP carrier in the mitochondrial membrane. The hydrophobicity of the maleimide derivatives ensures rapid spin-labeling on both sides of the mitochondrial membrane as well as in hydrophobic regions of the protein surface covered by phospholipids. Spin reduction by membrane-impermeable reducing agents represents an advantage of this labeling technique over the sulfhydryl labeling by radioactive NEM, since it allows the determination of the membrane sidedness of the spin-label binding sites. A similar experimental approach has been used by Houstek et al. (1983) in a study of the mitochondrial phosphate translocator.

The results of ESR double integration of MSL spectra after blocking by impermeable reagents (Table I) or after spin reduction (Table II) suggest that roughly half of the carrier-specific MSL binding sites are easily accessible from the cytosolic side of the mitochondrial membrane. It has been shown previously that the isolated ADP/ATP carrier in the m state can bind approximately two molecules of NEM in the dimeric protein molecule (Aquila et al., 1982a). More recently, Cys-56 was identified as a binding site of radioactive NEM (Boulay & Vignais, 1984). This result was obtained under labeling conditions yielding only about 70% of specific NEM incorporation. In the present spin-labeling experiments, the ratio of MSL to mitochondrial protein is similar to the NEM/protein ratios in the procedure of Boulay and Vignais (1984). Thus, one might expect that the spin-labeled maleimide will bind exclusively to the Cys-56 position in the amino acid sequence of the ADP/ATP carrier (Aquila et al., 1982a,b). Considering the dimeric structure of the carrier protein (Hackenberg & Klingenberg, 1980), this assumption leads to the conclusion that in the m state one of the carrier subunits exposes its Cys-56 residue to the matrix space, whereas in the other subunit this residue is directed to the cytosolic side.

It is usually assumed that a 2-fold symmetry axis normal to the membrane plane is characteristic of dimeric integral membrane proteins. Thus, the finding that after the c → m rearrangement SH groups in the AAC are exposed on both membrane sides suggests a perturbation of the principal molecular symmetry of the AAC dimer. This perturbation may be rationalized on the basis that only one ligand molecule such as ADP, ATP, or CAT and BKA bind to the dimeric AAC molecule. Since the dimer should potentially provide one center at each subunit, it might be assumed that binding of one ligand molecule induces an asymmetric conformational change within the dimer, such that the opposite monomer becomes nonbinding (Klingenberg, 1981).

These conclusions depend critically on the assumption that in mitochondria CAT suppresses exclusively maleimide binding to SH groups in the AAC. Shielding of SH groups in proteins other than AAC by CAT would lead to an overestimation of

the total percentage of AAC-specific SH groups (see Table I, spin density difference ± CAT). Similarly, unmasking of more than one SH group in each AAC subunit would give too high difference values. On the contrary, penetration of some DTNB during incubation could lead to partial blocking of carrier SH groups in the matrix space and thereby to a low difference value, as observed after preincubation with the membrane-permeable reagent NEM (see Table II). In any case, relaxation of the above proviso would lead to erroneous conclusions on the sidedness of the SH groups in the m state AAC.

Recently, Houstek and Pedersen (1985) concluded from studies with mitochondria and submitochondrial particles that eosin-5-maleimide labels the AAC exclusively on the matrix side of the mitochondrial membrane. However, these authors emphasized that eosin-5-maleimide and NEM are likely to label different SH groups in the AAC, since binding of eosin-5-maleimide was not suppressed by preincubation with NEM in submitochondrial particles. It can be assumed that the membrane permeable spin-labeled maleimides behave analogously to NEM rather than to the impermeable eosin-5-maleimide. Thus, the results obtained with the fluorescent label may not be directly comparable to the findings in the present study.

MSL Binding to the Solubilized Carrier Protein. In the titration experiments with Triton-solubilized AAC in the presence of BKA and ADP, about two to three CAT-sensitive MSL binding sites per protein molecule were found. This confirms that under the influence of ADP and BKA the solubilized protein assumes a conformation identical with the m state in the mitochondrial membrane. Experimentation with the isolated carrier affords additional information. First, it is possible to detect MSL binding to the CAT–carrier complex which is not discernible in mitochondria, due to the large background of foreign SH groups. Second, the mobility of the carrier-bound spin-labels may be deduced from the ESR line shape.

MSL binding to the CAT–carrier complex, ranging from 0.3 to 0.4 mol of MSL/ml of protein dimer, was observed consistently in all experiments. This "CAT-insensitive" binding was not remarkably distinguished by a different line shape from the MSL binding to the BKA–protein complex. Rather, s and w components were observed in the same proportion as in the BKA state. Thus, the CAT-insensitive binding cannot be attributed to only one of the two spectral components (see below).

These observations suggest that CAT-insensitive binding occurs due to a variable extent of protein denaturation. It should be remembered that in the present experiments the carrier is always transformed into the CAT or BKA states starting from the ATR–protein complex. This inhibitor exchange may result in slight protein damage since ATR stabilizes the carrier protein somewhat less than CAT.

The evaluation of spin-label mobility in the solubilized MSL–protein complex is hampered by the superposition of the s and w components. A reliable result may be obtained for MSL I (cf. Chart I and Figure 6) at 0 °C, considering only the s component. A rotational correlation time was deduced from the line widths of the low-field and high-field extrema as described by Freed (1976). Using a peak to peak derivative Lorentzian line width of 2.9 G, we obtained a correlation time of about 1×10^{-6} s. This is close to the correlation time to be expected for isotropic tumbling of the whole protein–detergent micelle, indicating very little segmental mobility of the spin-labeled maleimide.

Problem of Composite MSL Spectra. The two superimposed spectral components denoted by s and w were observed both in mitochondria and in the solubilized ADP/ATP carrier. In mitochondria, the possible contribution of MSL binding to soluble proteins in the mitochondrial matrix prevents a straightforward interpretation of the composite spectra. However, in the purified protein preparation, the s and w signals can be attributed exclusively to the ADP/ATP carrier. In this case, the components may originate from different MSL binding sites in the protein. However, the failure of all attempts to influence the s/w ratio strongly argues against separate spin-label binding sites. Also, the rather drastic change in the s/w ratio with increasing chain length of the spin-labels is difficult to explain on the basis of different binding sites.

As an alternative, it may be assumed that the bound spin-label exchanges between a mobile and a more immobilized state. Two spectral components can be expected, provided the exchange rate is sufficiently slow on the ESR time scale. The immobilized MSL component may reflect the interaction of the nitroxide moiety with amino acid residues on the protein surface. The increase in the w component with increasing spin-label length could be due to the enhanced population of the mobile state.

This interpretation bears resemblance to the transient immobilization of phospholipids in the vicinity of integral membrane proteins as detected by spin-label ESR (Marsh, 1985). Strong phospholipid binding in the detergent-solubilized AAC has been recently demonstrated by ^{31}P NMR (Beyer & Klingenberg, 1985). A two-component signal was also observed in ESR spectra of the spin-labeled inhibitor CAT (CATSL) when bound to the AAC (Munding et al., 1983). The experiments suggested that the weakly immobilized component was due to a second protein-bound CATSL portion.

The striking increase in the w signal amplitude when the maleimide–nitroxide distance transgresses 10 Å (see Figure 7) may be explained also in the context of this model, tentatively assuming that the spin-label is slowly exchanging between a mobile and an immobilized state. At a critical spacer length of 10 Å, the nitroxide moiety of the MSL molecule may no longer fit into the geometrical environment which provides the immobilizing binding site.

ACKNOWLEDGMENTS

We are grateful to Renate Lafuntal for excellent technical assistance.

REFERENCES

Aquila, H., & Klingenberg, M. (1979) in *Functions and Molecular Aspects of Biomembrane Transport* (Quagliariello, E., et al., Eds.) pp 305–308, Elsevier/North-Holland, Amsterdam.

Aquila, H., & Klingenberg, M. (1982) *Eur. J. Biochem. 122*, 141–145.

Aquila, H., Eiermann, W., & Klingenberg, M. (1982a) *Eur. J. Biochem. 122*, 133–139.

Aquila, H., Misra, D., Eulitz, M., & Klingenberg, M. (1982b) *Hoppe-Seyler's Z. Physiol. Chem. 363*, 345–349.

Beyer, K., & Klingenberg, M. (1985) *Biochemistry 24*, 3821–3826.

Blair, P. V. (1967) *Methods Enzymol. 10*, 78–81.

Bolton, J. R., Borg, D. C., & Swartz, H. M. (1972) in *Biological Applications of Electron Spin Resonance* (Swartz, H. M., Bolton, J. R., & Borg, D. C., Eds.) p 100, Wiley-Interscience, New York.

Boulay, F., & Vignais, P. V. (1984) *Biochemistry 23*, 4807-4812.
Erdelt, H., Weidemann, M. J., Buchholz, M., & Klingenberg, M. (1972) *Eur. J. Biochem. 30*, 107-122.
Freed, J. H. (1976) in *Spin Labeling I* (Berliner, L. J., Ed.) pp 53-133, Academic Press, New York.
Hackenberg, H., & Klingenberg, M. (1980) *Biochemistry 19*, 548-555.
Houstek, J., & Pedersen, P. L. (1985) *J. Biol. Chem. 260*, 6288-6295.
Houstek, J., Bertoli, E., Stipani, I., Pavelka, S., Megli, F. M., & Palmieri, F. (1983) *FEBS Lett. 154*, 185-190.
Hsia, J. C., & Piette, H. L. (1969) *Arch. Biochem. Biophys. 129*, 296-307.
Hull, H. H., Chang, R., & Kaplan, L. J. (1975) *Biochim. Biophys. Acta 400*, 132-136.
Klingenberg, M. (1975) *Eur. J. Biochem. 52*, 351-363.
Klingenberg, M. (1976) *Eur. J. Biochem. 65*, 601-605.
Klingenberg, M. (1981) *Nature (London) 290*, 449-454.
Klingenberg, M., Riccio, P., Aquila, H., Buchanan, B. B., & Grebe, K. (1976) in *The Structural Basis of Membrane Function* (Hatefi, J., & Djavadi-Ohaniance, L., Eds.) pp 293-311, Academic Press, New York.
Leblanc, P., & Clauser, H. (1972) *FEBS Lett. 23*, 107-113.
Marsh, D. (1985) in *Progress in Protein-Lipid Interactions* (Watts, A., & DePont, J. F. H. H. M., Eds.) Vol. 1, pp 143-172, Elsevier, Amsterdam.
Müller, M., Krebs, J. J. R., Cherry, R. J., & Kawato, S. (1984) *J. Biol. Chem. 259*, 3037-3043.
Munding, A., Beyer, K., & Klingenberg, M. (1983) *Biochemistry 22*, 1941-1947.
Reed, H. C., & Bygrave, F. L. (1974) *Biochem. J. 140*, 143-155.
Rozantsev, E. G. (1970) *Free Nitroxyl Radicals* (translated by B. J. Hazzard) Plenum Press, New York.
Vignais, P. M., Chabert, J., & Vignais, P. V. (1974) *FEBS-Symp. 35*, 307-313.
Vignais, P. V., & Vignais, P. M. (1972) *FEBS Lett. 26*, 27-31.
Weidemann, M. J., Erdelt, H., & Klingenberg, M. (1969) in *Inhibitors: Tools in Cell Research* (Bücher, Th., & Sies, H., Eds.) pp 324-334, Springer Verlag, Berlin/Heidelberg/New York.
Zeidan, H., Han, P., & Johnson, J. (1985) *FEBS Lett. 192*, 294-298.

Antenna Organization in Green Photosynthetic Bacteria. 1. Oligomeric Bacteriochlorophyll *c* as a Model for the 740 nm Absorbing Bacteriochlorophyll *c* in *Chloroflexus aurantiacus* Chlorosomes†

Daniel C. Brune, Tsunenori Nozawa,‡ and Robert E. Blankenship*
Department of Chemistry, Arizona State University, Tempe, Arizona 85287-1604
Received May 15, 1987; Revised Manuscript Received August 25, 1987

ABSTRACT: Bacteriochlorophyll (BChl) *c* was extracted from *Chloroflexus aurantiacus* and purified by reverse-phase high-pressure liquid chromatography. This pigment consists of a complex mixture of homologues, the major component of which is 4-ethyl-5-methylbacteriochlorophyll *c* stearyl ester. Unlike previously characterized BChls *c*, the pigment from *C. aurantiacus* is a racemic mixture of diastereoisomers with different configurations at the 2a chiral center. Diluting a concentrated methylene chloride solution of BChl *c* with hexane produces an oligomer with absorption maxima at 740–742 and at 460–462 nm. Both the absorption spectrum and the fluorescence emission spectrum (maximum at 750 nm) of this oligomer closely match those of BChl *c* in chlorosomes. Further support for this model comes from the ability of alcohols, which disrupt BChl *c* oligomers by ligating the central Mg atom, to convert BChl *c* in chlorosomes to a monomeric form when added in low concentrations. The lifetime of fluorescence from the 740 nm absorbing BChl *c* oligomer is about 80 ps. Although exciton quenching might be unusually fast in the in vitro BChl *c* oligomer because of its large size and/or the presence of minor impurities, this result suggests that energy transfer from the BChl *c* antenna in chlorosomes must be very fast if it is to be efficient.

Bacteriochlorophyll (BChl)[1] *c* is a family of green pigments that occur only in green photosynthetic bacteria. These pigments resemble pyrochlorophyll *a* in being 7,8-dihydroporphyrins that have a central Mg atom but lack a 10-(carboxymethyl) group. Although its synthesis is repressed at high light intensities, BChl *c* is usually the major chlorophyll in green bacteria and can constitute 90–95% of the total, the rest being BChl *a* (Pierson & Castenholz, 1978; Olson, 1980). Except in the case of green sulfur bacteria (Chlorobiaceae), in which a small portion of the BChl *c* (or a structurally modified form) appears to function as the primary electron acceptor (Nuijs et al., 1985; Braumann et al., 1985), all of the BChl *c* occurs in chlorosomes, antenna structures attached

† This work was supported by a grant to R.E.B. from the Biological Energy Storage Division of the U.S. Department of Energy and by a grant to T.N. from the Japanese Ministry of Education (Japan–U.S. Cooperative Photoconversion and Photosynthesis Research Program). Funds for purchasing the NMR spectrometer were provided by ASU and by NSF Grant CHE 8409644. The Center for Fast Kinetics Research is supported jointly by the Biomedical Research Technology Program of the Division of Research Resources of NIH (RR 00886) and by the University of Texas at Austin.
* Address correspondence to this author.
‡ Permanent address: Chemical Research Institute of Non-aqueous Solutions, Tohoku University, Sendai 980, Japan.

[1] Abbreviations: BChl, bacteriochlorophyll; BPh, bacteriopheophytin; *C., Chloroflexus*; Chl, chlorophyll; HPLC, high-pressure liquid chromatography; NMR, nuclear magnetic resonance; Tris-HCl, tris(hydroxymethyl)aminomethane hydrochloride.

0006-2960/87/0426-8644$01.50/0